DOI: 10.1002/ange.201209809

Biomass

Tungsten-Based Catalysts for Selective Deoxygenation**

*Robert W. Gosselink, Daniel R. Stellwagen, and Johannes H. Bitter**

Over the past decades, impending oil shortages combined with petroleum market instability have prompted a search for a new source of both transportation fuels and bulk chemicals. Renewable bio-based feedstocks such as sugars, grains, and seeds are assumed to be capable of contributing to a significant extent as fuel and bulk chemical sources.[1] However, utilization of these new types of high-oxygen-content feeds as either fuels or bulk chemical precursors is not trivial. Triglyceride or fatty acid feeds have the potential to be used as fuel because of their structural resemblance to diesel-type hydrocarbons, but further processing is required to reduce their high-oxygen content and related acidity.[2] This goal is typically achieved by hydroprocessing, thus resulting in deoxygenation (DO) of the triglyceride/fatty acid feed and yielding either saturated hydrocarbons suitable for diesel fuel, or linear olefins suitable for bulk chemical precursors.

Although extensive studies have been done on deoxygenation of biomass-related feeds,[2,3] catalyst research has so far been limited to supported noble-metal catalysts known for their hydrogenation activity and standard hydrodesulfurization (HDS) catalysts. The use of HDS catalysts can be problematic since catalyst deactivation resulting from sulfur leaching will result in contamination of the product stream.[4] The major drawback of noble-metal catalysts is their limited availability. Herein we demonstrate the use of tungsten-based catalysts for the deoxygenation of triglyceride-based feedstocks. Changes in a (pre)treatment procedure are shown to control catalyst selectivity, thus allowing high yields of unsaturated products even in the presence of hydrogen.

Deoxygenation of biomass-derived glyceride feeds can occur by different pathways depending on reaction conditions and the type of catalyst used. The different pathways for the deoxygenation of fatty acids are given in Scheme 1. Decarbonylation and decarboxylation [DCO, Equations (1) and (2)] yield hydrocarbon chains with one carbon atom less as compared to the reactant. Decarbonylation yields olefins and decarboxylation produces paraffins. Hydrodeoxygenation [HDO, Equation (3)] results in hydrocarbons with the same chain length as the starting compound.[3,5]

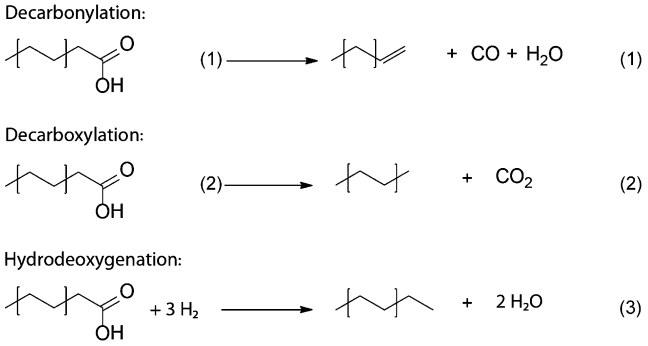

Scheme 1. Pathways for the deoxygenation of fatty acids.

Aiming to develop a catalyst that provides the means to achieve better control over the various competing reactions in the deoxygenation process, we have studied the deoxygenation of several model compounds (stearic acid, methyl stearate, and tristearin) over carbon-supported tungsten-based catalysts.

Tungsten-based materials are known to be versatile catalysts with various applications ranging from acid catalysis by tungsten oxides[6] to hydrogenation by tungsten carbides.[7] Carbon-supported (sulfided) tungsten oxide was reported to be a potent catalyst in the HDS process.[8,9] Bulk tungsten monocarbide (WC) showed hydrodenitrogenation (HDN) activities comparable to that of a commercial sulfided NiMo/Al_2O_3 catalyst.[8] Although the performance of tungsten-based catalysts in the HDS and HDN processes is promising, so far these catalysts have not yet been able to achieve similar success in deoxygenation reactions. As the electronic structure and reactivity of tungsten-based catalysts is highly susceptible to minor phase changes,[10] controlling these phase transitions is likely to be an essential part of tungsten-based catalyst design.[11–13]

To facilitate synthetic control over the tungsten phase, all catalysts in our work were supported on carbon and prepared by carbothermal reduction.[14] Carbon nanofibers (CNFs) were used as the support. CNFs are eminently suitable for such a purpose because of their high surface area and mesoporosity.[15,16] Several W-oxide- and W-carbide-based deoxygenation catalysts were prepared by incipient wetness impregnation of the CNF support with aqueous ammonium metatungstate. Next, a heat treatment under an inert atmosphere was applied at temperatures ranging from 600 to 1000 °C to obtain the desired tungsten phase. Characteristics of the catalysts used in this work are summarized in Table 1 and discussed below.

[*] R. W. Gosselink,[+] D. R. Stellwagen,[+] Dr. J. H. Bitter
Department of Inorganic Chemistry and Catalysis
Utrecht University
Universiteitsweg 99, 3584CG, Utrecht (The Netherlands)
E-mail: J.H.Bitter@uu.nl
Homepage: http://www.anorg.chem.uu.nl

[+] These authors contributed equally to this work.

[**] This research has been performed within the framework of the CatchBio program. We gratefully acknowledge the support of the Smart Mix Program of the Netherlands Ministry of Economic Affairs and the Netherlands Ministry of Education, Culture, and Science. Philip Walder is kindly acknowledged for the equipment preparation and initial experiments. We thank Lucian Roiban for the TEM measurements, Jesper Sättler for his help during Raman analysis, and Krijn de Jong for discussions and suggestions.

Supporting information for this article is available on the WWW under http://dx.doi.org/10.1002/anie.201209809.

Table 1: Characteristics of tungsten/CNF-based catalysts.

Sample[a]	T[a] [°C]	Tungsten phase[b]	Particle size [nm][c]	BET [$m^2 g^{-1}$]
W-600	600	WO_3	3.8	144
W-700	700	$WO_3 + WO_x$[e]	4.6	140
W-800	800	WO_x[e] + WO_2 + W_2C	4.4	135
W-900	900	WO_2 + W_2C	4.1	129
W-1000	1000	W_2C	4.0	118
CNF	120	–	–	180

[a] Heat treatment temperature. [b] From XRD. [c] Average from XRD (from Scherrer equation) confirmed with TEM. [d] From N_2 physisorption. [e] $2 < x < 3$.

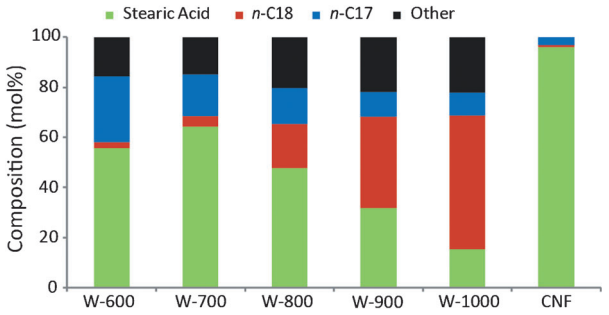

Figure 1. Composition of the reaction mixture after the deoxygenation of stearic acid by various tungsten-based catalysts. Bare CNFs are included as a reference. Reaction conditions: $T = 350$ °C, $p = 50$ bar H_2, $t = 5$ h, $m_{\text{stearic acid}} = 2$ g, $m_{\text{cat}} = 0.25$ g, $m_{\text{dodecane}} = 36$ g.

The XRD results shown in Figure S1 and Table S1 of the Supporting Information indicate that tungsten trioxide formation starts at 600 °C, after which partial reduction and carburization of the WO_3 crystallites by the CNF support occurs at 700–1000 °C. The tungsten carbide phase becomes dominant at 900 °C and eventually phase-pure supported W_2C is formed at 1000 °C. This reduction/carburization pathway is consistent with previous studies on the carbothermal reduction of tungsten oxide by carbon supports under an inert atmosphere.[17–19] XRD and TEM data indicate that the average crystallite size was approximately 4 nm for all samples. Typical TEM images for supported tungsten oxide (W-600) and supported tungsten carbide (W-1000) are shown in Figure S2 of the Supporting Information. With increasing heat treatment temperature, an increase in particle size is typically expected because of sintering effects, but this is not observed in this case. It appears that the sintering of tungsten oxide crystallites is negated by the break-up of larger crystallites by partial reduction and subsequent carburization in a competing process.

The samples were further analyzed with Raman spectroscopy (see Figure S3 in the Supporting Information). The presence of various tungsten oxides in the W-600 and W-700 catalysts was observed, and was in agreement with the XRD results shown above. Also, the near constant ratio of the D,G peaks at 1340 and 1570 cm^{-1} show that the graphitic structure of the CNF was retained even under carburizing conditions (W-900 and W-1000).

The tungsten-based catalysts were initially tested for the deoxygenation of stearic acid (Figure 1). The deoxygenation product yields (*n*-C17 and *n*-C18) are plotted together with other products formed in side reactions such as cracking and formation of oxygenates, which are known to occur under these reaction conditions.[3] A more detailed overview of the product selectivities can be found in Table S2 and Figure S4 in the Supporting Information. Bare CNFs have a negligible deoxygenation yield (< 5 %). The tungsten-oxide-based catalysts (W-600, W-700) show high selectivity for *n*-C17 hydrocarbons, which are formed by DCO (Scheme 1). The tungsten-carbide-based catalysts (W-900 and W-1000) are highly selective for *n*-C18 hydrocarbons, which are formed by the HDO mechanism (Scheme 1). The W-800 catalyst, containing both tungsten oxide and tungsten carbide phases, shows comparable *n*-C17 and *n*-C18 hydrocarbon selectivity. The selectivity of the catalysts in the deoxygenation of stearic acid appears closely correlated to the dominant tungsten phase present. This correlation was further confirmed in experiments with bulk WO_3 and W_2C catalysts (see Table S3 in the Supporting Information), where similar trends in selectivity were observed, that is, WO_3 is selective for *n*-C17 products and W_2C is selective for *n*-C18 products.

The versatility of the CNF-supported tungsten catalysts is illustrated by recycle tests of the catalysts (see Figure S5 in the Supporting Information). When the spent W-600, selective for DCO, was regenerated at 1000 °C (forming W_2C phase) and retested, a full switch in product selectivity to HDO was observed. The spent catalyst from this second experiment could again be regenerated (forming WO_3) to revert to the original W-600-product selectivity. This series of experiments shows that catalyst selectivity can be varied as desired upon heat treatment. Reusability tests (see Table S5 in the Supporting Information) without intermediate switching of the tungsten phase show a slight loss in activity for the W-600 catalyst resulting from sintering of the active phase, whereas the W-1000 catalyst could be reused without loss of activity.

To gain more insight into the sequence of product formation during the deoxygenation process, the evolution of products over W-600 and W-1000 as a function of time was investigated. The product yields are shown in Figure 2. For W-600 (Figure 2 A) a simultaneous evolution of heptadecane (decarboxylation product) and heptadecene (decarbonylation product) was observed, thus indicating that both reactions occur in parallel. Initially the concentration of heptadecene is higher than that of heptadecane, thereby indicating the decarbonylation pathway is preferred. At longer reaction times the heptadecene yield gradually decreases while heptadecane becomes the main product. This can be explained by hydrogenation of the unsaturated hydrocarbon products occurring alongside the decarboxylation and decarbonylation processes. Trace amounts (< 2 %) of the *n*-C18 hydrocarbon HDO products were also detected in the W-600-catalyzed reaction (see also Table S2). For W-1000 (Figure 2 B) a high selectivity toward the unsaturated HDO product octadecene was initially observed, while the octadecane content was negligible. However, at long reaction times octadecane is observed as the only *n*-C18 product, thus pointing to a sequential reaction mechanism in which the alkene is the initial reaction product, which is then hydro-

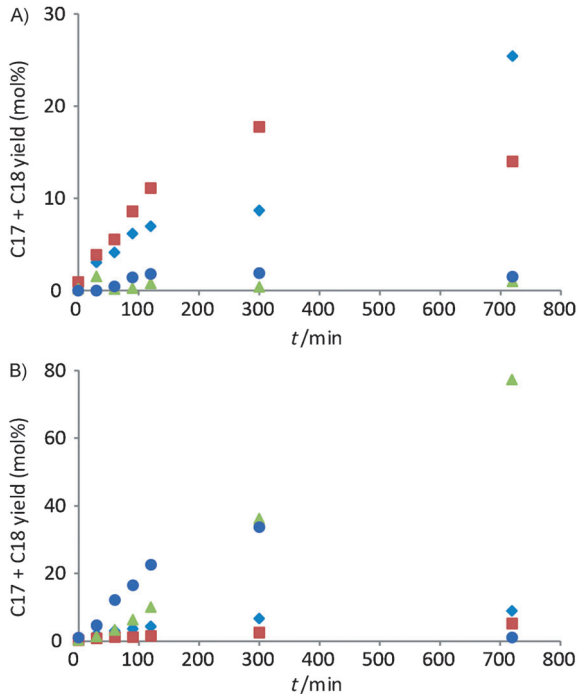

Figure 2. *n*-C17 and *n*-C18 hydrocarbon yields over time for W-600 (A) and W-1000 (B): Heptadecane (red), heptadecene (blue), octadecane (green), and octadecene (purple). Reaction conditions: $T = 350\,°C$, $p = 50$ bar H_2, $m_{\text{stearic acid}} = 2$ g, $m_{\text{cat}} = 0.25$ g, $m_{\text{dodecane}} = 36$ g.

genated in a slower second step. This is in accordance with a mechanism previously proposed for the HDO of methyl-dodecanoate to dodecane by $NiMo/Al_2O_3$, in which 1-dodecene was observed as a primary product and hydrogenation of the double bond was regarded as the rate-limiting step.[5] It should be noted that small amounts (< 10 %) of *n*-C17 hydrocarbons were also obtained, thus indicating the presence of surface WO_x species formed by partial oxidation of the tungsten carbide surface upon contact with air.[11–13]

The catalytic deoxygenation of stearic acid with W-1000 also revealed trace amounts (< 2 %) of stearyl alcohol and octadecanal in the product mixture. These products were not observed in the W-600-catalyzed reaction. Based on this observation we performed reactivity studies with these potential intermediates under the reaction conditions using both our tungsten-oxide- and tungsten-carbide-based catalysts to gain more information on the role of these tungsten phases in catalysis.

The results are shown in Scheme 2 and Table S4 in the Supporting Information. We propose that acidic tungsten oxide surface sites promote dehydration to **2** and decarboxylation to **3**, whereas the reported ability of tungsten carbide sites to chemisorb hydrogen promotes the hydrodeoxygenation process (**4**–**8**).[11,20] The intermediates **4** and **7** do not appear in the WO_3/CNF-catalyzed deoxygenation of stearic acid.

The tungsten-based catalysts were also tested for the deoxygenation of other fat/oil model compounds, methyl-stearate and tristearin. The results of these experiments are compiled in Table 2. W-600 shows similar reactant conversion

Table 2: The catalytic activity for the (hydro)deoxygenation of various model compounds. Reaction conditions: $T = 350\,°C$, $p = 50$ bar H_2, $p = 5$ h, $p_{\text{reactant}} = 2$ g, $p_{\text{cat}} = 0.25$ g, $p_{\text{dodecane}} = 36$ g.

Feed[a]	Catalyst	Conv. [%]	DO Selectivity[b]	HDO/DCO[c]
SA	W-600	38	80	9:91
SA	W-1000	81	83	85:15
MS	W-600	42	60	11:89
MS	W-1000	100	96	97:3
TS	W-600	47	54	10:90
TS	W-1000	100	90	86:14
MM	W-600	45	59	12:88
MM	W-1000	100	84	91:9

[a] SA = stearic acid; MS = methyl stearate; TS = tristearin; MM = Model Mix (5 % tristearin, 20 % stearic acid, 5 % methyl stearate). [b] Selectivity for deoxygenation products. [c] Ratios of hydrodeoxygenation and decarboxylation/decarbonylation products.

levels for the three model compounds, that is, 40–45 %. Since DO selectivity is below 100 %, it must be concluded that other side reactions occur as well. As shown in Table S6 in the Supporting Information, these side reactions can be attributed to cracking, which is known to occur under these reaction conditions.[3] The tendency to form undesired side products is significantly reduced for W-1000, and is in accordance with the stearic acid deoxygenation results on W-600 and W-1000 (Figure 2 and Table S2). Large differences in HDO to DCO selectivities are once again observed for the two tungsten-based catalysts. The W_2C phase catalyzes the HDO pathway whereas DCO products are highly dominant for the WO_3 catalyst. The data in Table 2 also show that W-600 mainly produces olefins, whereas the W-1000 catalyst tends to yield paraffins because of the high conversion at the chosen reaction times. The olefin products are dominant at shorter reaction times (results not shown), and is similar to the results found for stearic acid (Figure 2B). Finally, a mixture of the fat/oil model

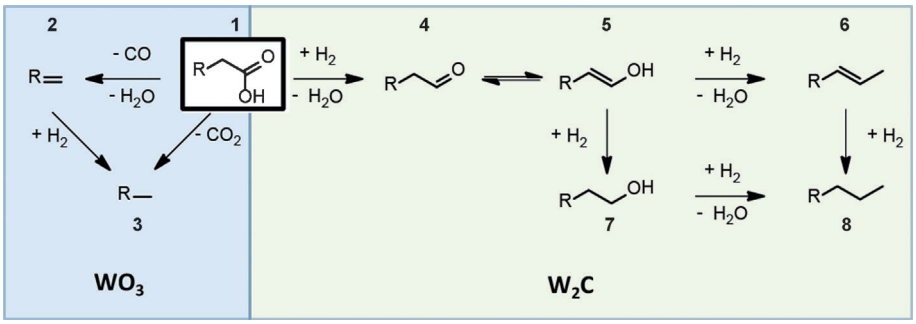

Scheme 2. Stearic acid conversion pathways catalyzed by tungsten oxide and tungsten carbide.

compounds was also tested in a ratio comparable to vegetable oils. The expected selectivities for both W-600 and W-1000 were obtained, that is, mainly DCO products for WO_3/CNF and HDO products for the W_2C/CNF catalyst.

In summary, carbon-supported tungsten-based materials are presented as a novel catalyst for the deoxygenation of biomass-derived glyceride feeds. Supported tungsten oxides were shown to be selective toward decarboxylation/decarbonylation products, whereas supported tungsten carbide was selective towards hydrodeoxygenation products. In both cases high yields of unsaturated hydrocarbons could be obtained from a glyceride feed with saturated hydrocarbon chains, thus allowing an upgrade of the feed to higher-value products, even in the presence of H_2.

Experimental Section

CNFs were prepared according to literature.[21] The support was then impregnated using ammonium metatungstate (Aldrich) by pore volume (0.7 mL g^{-1} determined by water uptake) impregnation and dried under vacuum at 80 °C for 24 h to obtain a 15 wt % W. Subsequently heat treatments were applied at different temperatures (600–1000 °C) under N_2 atmosphere based on the desired tungsten phase for 3 h. The samples are denoted as W-*x*, where *x* is the temperature.

N_2-physisorption isotherms were recorded with a Micromeritics Tristar 3000 at 77 K. The surface area was determined using the Brunauer-Emmett-Teller (BET) theory.[22] X-ray powder diffraction (XRD) patterns were obtained by a Bruker-AXS D2 Phaser powder X-ray diffractometer using Co $K_{\alpha1,2}$ with $k = 1.79026$. Measurements were carried out between 10 and 100°2θ using a step size of 0.09 2θ and a scan speed of 1 s.

Raman spectroscopy was performed using a Kaiser Optical Systems Inc. Raman Spectrometer equipped with a 532 nm laser. Measurements were done at 50 mW with an exposure time of 7 s and 11 accumulations using Holograms 4.0 software.

TEM analysis was performed using a FEI TECNAI20F Transmission.

Electron microscope operated at 200 keV. Catalytic experiments were carried out in a 100 mL EZE Autoclave Engineer Batch reactor. After loading of the reactor with 0.25 g catalyst, 2 g reactant, 1 g tetradecane (internal standard) and 50 mL of dodecane as solvent, the reactor was pressurized with 50 bar H_2 and reaction was subsequently run at 350 °C whilst stirring with 1000 rpm. The reaction was quenched after the desired reaction time with an ice bath. Reaction mixture work up was performed with a $CHCl_3$/MeOH (2:1) mixture that was heated to 40 °C to ensure complete dissolution of the stearic acid. A sample was subsequently taken from the mixture and methylated using trimethylsulfonium hydroxide for GC analysis.[23]

Received: December 7, 2012
Revised: February 14, 2013
Published online: April 3, 2013

Keywords: biomass · nanostructures · olefins · supported catalysts · tungsten

[1] G. W. Huber, S. Iborra, A. Corma, *Chem. Rev.* **2006**, *106*, 4044 – 4098.
[2] E. Furimsky, *Appl. Catal. A* **2000**, *199*, 147 – 190.
[3] M. Snåre, I. Kubičková, P. Mäki-Arvela, K. Eränen, D. Y. Murzin, *Ind. Eng. Chem. Res.* **2006**, *45*, 5708 – 5715.
[4] O. I. Şenol, E. M. Ryymin, T. R. Viljava, A. O. I. Krause, *J. Mol. Catal. A* **2007**, *268*, 1 – 8.
[5] B. Donnis, R. G. Egeberg, P. Blom, K. G. Knudsen, *Top. Catal.* **2009**, *52*, 229 – 240.
[6] D. G. Barton, S. L. Soled, E. Iglesia, *Top. Catal.* **1998**, *6*, 87 – 99.
[7] R. B. Levy, M. Boudart, *Science* **1973**, *181*, 547 – 549.
[8] B. Pawelec, R. Mariscal, J. L. G. Fierro, A. Greenwood, P. T. Vasudevan, *Appl. Catal. A* **2001**, *206*, 295 – 307.
[9] S. Ramanathan, S. T. Oyama, *J. Phys. Chem.* **1995**, *99*, 16365 – 16372.
[10] V. P. Zhukov, V. A. Gubanov, *Solid State Commun.* **1985**, *56*, 51 – 55.
[11] E. Iglesia, F. H. Ribeiro, M. Boudart, J. E. Baumgartner, *Catal. Today* **1992**, *15*, 307 – 337.
[12] F. Ribeiro, R. A. Dalla Betta, M. Boudart, J. Baumgarner, E. Iglesia, *J. Catal.* **1991**, *130*, 86 – 105.
[13] F. Ribeiro, M. Boudart, R. A. Dalla Betta, E. Iglesia, *J. Catal.* **1991**, *130*, 498 – 513.
[14] M. A. Alvarez-Merino, F. Carrasco-Marin, J. L. G. Fierro, C. Moreno-Castilla, *J. Catal.* **2000**, *192*, 363 – 373.
[15] J. H. Bitter, *J. Mater. Chem.* **2010**, *20*, 7312 – 7321.
[16] K. P. de Jong, J. W. Geus, *Catal. Rev. Sci. Eng.* **2000**, *42*, 481 – 510.
[17] D. S. Venables, M. E. Brown, *Thermochim. Acta* **1996**, *282/283*, 251 – 264.
[18] D. S. Venables, M. E. Brown, *Thermochim. Acta* **1996**, *282/283*, 265 – 276.
[19] M. A. Alvarez-Merino, M. F. Ribeiro, J. M. Silva, F. Carrasco-Marin, F. J. Maldonado-Hódar, *Environ. Sci. Technol.* **2004**, *38*, 4664 – 4670.
[20] J. Han, J. Duan, P. Chen, H. Lou, X. Zheng, *Adv. Synth. Catal.* **2011**, *353*, 2577 – 2583.
[21] M. L. Toebes, M. K. van der Lee, L. M. Tang, M. H. Huis in't Veld, J. H. Bitter, J. van Dillen, K. P. de Jong, *J. Phys. Chem. B* **2004**, *108*, 11611.
[22] S. Brunauer, P. H. Emmett, E. Teller, *J. Am. Chem. Soc.* **1938**, *60*, 309.
[23] W. Butte, *J. Chrom.* **1983**, *261*, 142 – 145.
[24] ICDD PDF-2 database package http://www.icdd.com/products/pdf2.htm.
[25] S. S. Chan, I. E. Wachs, L. L. Murrell, *J. Catal.* **1984**, *90*, 150 – 155.
[26] M. Boulova, G. Lucazeau, *J. Solid State Chem.* **2002**, *167*, 425 – 434.
[27] I. E. Wachs, *Catal. Today* **1996**, *27*, 437 – 455.
[28] E. I. Ross-Medgaarden, I. E. Wachs, *J. Phys. Chem. C* **2007**, *111*, 15089 – 15099.
[29] D. G. Barton, M. Shtein, R. D. Wilson, S. L. Soled, E. Iglesia, *J. Phys. Chem. B* **1999**, *103*, 630 – 640.
[30] S. S. Chan, I. E. Wachs, L. L. Murrell, N. C. Dispenziere, Jr., *J. Catal.* **1985**, *92*, 1 – 10.
[31] A. Sadezky, H. Muckenhuber, H. Grothe, R. Niessner, U. Pöschl, *Carbon* **2005**, *43*, 1731 – 1742.
[32] B. Peng, Y. Yao, C. Zhao, J. A. Lercher, *Angew. Chem.* **2012**, *124*, 2114 – 2117; *Angew. Chem. Int. Ed.* **2012**, *51*, 2072 – 2075.
[33] W. O. Haag, R. M. Lago, P. B. Weisz, *Faraday Discuss. Chem. Soc.* **1981**, *72*, 317 – 330.
[34] A. Corma, A. V. Orchillés, *Microporous Mesoporous Mater.* **2000**, *35 – 36*, 21 – 30.
[35] B. Peng, X. Yuan, C. Zhao, A. Lercher, *J. Am. Chem. Soc.* **2012**, *134*, 9400 – 9405.
[36] D. Kubička, M. Bejblová, J. Vlk, *Top. Catal.* **2010**, *53*, 168 – 178.
[37] M. Snåre, I. Kubičková, P. Mäki-Arvela, K. Eranen, J. Warna, D. Y. Murzin, *Chem. Eng. J.* **2007**, *134*, 29 – 34.
[38] M. Snåre, I. Kubičková, P. Mäki-Arvela, D. Chichova, K. Eranen, D. Y. Murzin, *Fuel* **2008**, *87*, 933 – 945.

